Population transfer and quantum entanglement implemented in cold atoms involving two Rydberg states via an adiabatic passage

Xue-Dong Tian,[1,2] Yi-Mou Liu,[2] Cui-Li Cui,[1] and Jin-Hui Wu[2,*]

[1]*College of Physics, Jilin University, Changchun 130012, People's Republic of China*

[2]*Center for Quantum Sciences, Northeast Normal University, Changchun 130117, People's Republic of China*

(Received 29 September 2015; published 14 December 2015)

We study the adiabatic passage for a pair of interacting cold atoms driven into the ladder configuration with one ground state and two Rydberg states. We find, with proper single-photon and two-photon detunings, that it is viable to (i) achieve efficient population transfer from the ground state to either Rydberg state by fully overcoming the dipole blockade effect and (ii) implement maximal entangled states by partially overcoming the dipole blockade effect. These entangled atomic states are very stable and have purities and fidelities approaching 100%, among which one is of particular interest since it involves the simultaneous excitation of two different Rydberg states.

DOI: 10.1103/PhysRevA.92.063411 PACS number(s): 32.80.Rm, 32.80.Ee, 03.67.Bg, 03.65.Ud

I. INTRODUCTION

Stimulated Raman adiabatic passage (STIRAP) is an efficient technique utilizing partially overlapping pulses to produce the complete population transfer between two quantum states of an atom or molecule [1]. Applications of this technique are broad, not only to accurate preparation of selected states for reaction studies but also to many aspects of quantum optics and atom optics. Quite recently, the STIRAP technique has been adopted to attain efficient population transfer from one of the lowest ground states to a high-lying Rydberg state [2–4]. Compared to the general atomic excitations, strong interatomic interactions induced by huge dipole moments of Rydberg states may result in very poor effects of pumping strategies in the Rydberg excitation. That is, dipole-dipole interactions (DDI) can shift a Rydberg state out of resonance and then block its excitation when one neighboring atom has been excited to this Rydberg state. This is the essence of the so-called Rydberg blockade effect [5–12]. Increasing the mean interatomic distance (typically larger than 10 μm) by lowering the atomic density [13] and utilizing an appropriate optical detuning with respect to one Rydberg state to compensate its dipole-induced energy shift [2,14–16] are two feasible ways to overcome the obstacle of a desired Rydberg excitation.

Quantum entanglement and quantum gates are vital resources in most applications of quantum information science, so they have become the subjects of broad theoretical interest, and their experimental implementations have been demonstrated in various physical systems. In particular, some schemes utilizing large dipole moments of highly excited Rydberg states have been implemented for creating quantum gates [17–25] and entanglement [2,26–29]. Among these endeavors, a few proposals have been made to combine STIRAP and DDI [2,21,23,25]. So far most such schemes or proposals consider various level configurations with a single Rydberg state, whereas those involving two or more Rydberg states [30–32], in which we may find much richer nonlinear phenomena, have been rarely touched owing to more complicated dipole-dipole interactions between different Rydberg states.

Here we focus on a pair of cold atoms driven by two coherent fields to the ladder configuration with one ground state $|g\rangle$, one lower Rydberg state $|e\rangle$, and one higher Rydberg state $|r\rangle$. With strong interatomic interactions, the excitation to either Rydberg state is largely suppressed in general due to dipole blockade, so that both atoms stay in the ground state for resonant pumping. But we find that efficient population transfer between the ground state and one Rydberg state and reliable entanglement generation involving two of the three atomic states can be attained by modulating both single-photon and two-photon detunings of the applied fields. The underlying physics is that efficient population transfer (reliable entanglement generation) becomes viable when the level shift of one Rydberg state caused by dipole-dipole interactions is suitably compensated as a result of the complete (partial) antiblockade effect. It is worth noting that the four attainable maximal entangled states [$1/\sqrt{2}(|ge\rangle + |eg\rangle)$, $1/\sqrt{2}(|gr\rangle + |rg\rangle)$, $1/\sqrt{2}(|er\rangle + |re\rangle)$, and $1/\sqrt{2}(|gg\rangle - |ee\rangle)$] are very stable because the Rydberg states are also long-lived, and the one involving both Rydberg states may be explored to yield deterministic photon pairs. Last but not least, the fidelities and purities of these entangled states could approach 100% after a careful parameter optimization.

II. MODEL AND EQUATIONS

We consider a pair of cold atoms (e.g., in dipole traps) with a ground state $|g\rangle$ and two high Rydberg states $|e\rangle$ and $|r\rangle$ in the ladder configuration, as shown in Fig. 1(a). State $|e\rangle$ is connected by an optical pumping field of Rabi frequency Ω_p and a microwave coupling field of Rabi frequency Ω_c to state $|g\rangle$ and state $|r\rangle$, respectively. The optical pumping from state $|g\rangle$ to state $|e\rangle$ can be either a single-photon process [33] or a two-photon process via a highly detuned intermediate state [19,34]. Both $|e\rangle$ and $|r\rangle$ are long-lived excited states and typically have small decay rates Γ_e and Γ_r of the order of kilohertz. If these two trapped atoms occupy the same Rydberg state $|e\rangle$ ($|r\rangle$), they will interact via the van der Waals (vdW) potential $\mathcal{V}_{ee} = \hbar(C_6^{ee}/R^6)|e_A\rangle\langle e_A| \otimes$

*Corresponding author: jhwu@nenu.edu.cn

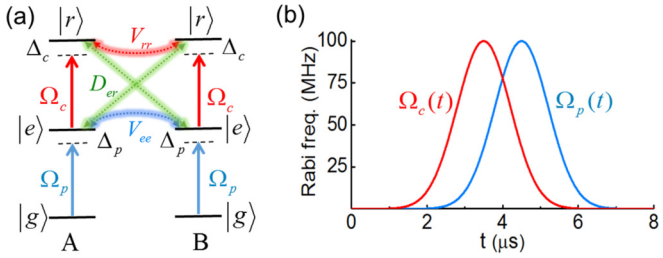

FIG. 1. (Color online) (a) Schematic representation of two cold atoms interacting via van der Waals (V_{ee} and V_{rr}) and dipole-dipole (D_{er}) potentials. The lowest state $|g\rangle$ is coupled by an optical field of Rabi frequency Ω_p and detuning Δ_p to the intermediate state $|e\rangle$, which is further coupled by a microwave field of Rabi frequency Ω_c and detuning Δ_c to the highest state $|r\rangle$. (b) An illustration of the counterintuitive sequence for pulses $\Omega_p(t)$ and $\Omega_c(t)$ of Gaussian profiles.

$|e_B\rangle\langle e_B|$ [$\mathcal{V}_{rr} = \hbar(C_6^{rr}/R^6)|r_A\rangle\langle r_A| \otimes |r_B\rangle\langle r_B|$], with R being the interatomic distance and C_6^{ee} and C_6^{rr} being the corresponding vdW coefficients. But if these two trapped atoms occupy different Rydberg states, they will experience instead the resonant dipole-dipole interaction $\mathcal{D}_{er} = \hbar(C_3^{er}/R^3)(|e_A\rangle\langle r_A| \otimes |r_B\rangle\langle e_B| + |r_A\rangle\langle e_A| \otimes |e_B\rangle\langle r_B|)$, with C_3^{er} being the corresponding DDI coefficient. With the above considerations, it is then straightforward to write down the following interaction Hamiltonian:

$$\mathcal{H} = \mathcal{H}_A \otimes I + I \otimes \mathcal{H}_B + \mathcal{V}_{ee} + \mathcal{V}_{rr} + \mathcal{D}_{er}, \tag{1}$$

with single-atom Hamiltonians

$$\begin{aligned}\mathcal{H}_i = &-\hbar[\Delta_p|e\rangle\langle e| + \Delta|r\rangle\langle r|] \\ &- \hbar(\Omega_p|e\rangle\langle g| + \Omega_c|r\rangle\langle e| + \text{H.c.})\end{aligned} \tag{2}$$

for $i = A,B$. Here Δ_p and Δ_c denote the single-photon detunings, while $\Delta = \Delta_p + \Delta_c$ is the two-photon detuning for the pumping and coupling fields.

The dynamic evolution of this two-atom system is governed as usual by the master equation

$$\begin{aligned}\frac{\partial\rho}{\partial t} = &-\frac{i}{\hbar}[\mathcal{H},\rho] + \sum_{j,k} C_k^{(j)}\rho C_k^{(j)\dagger} \\ &- \frac{1}{2}\sum_{j,k}\left(C_k^{(j)\dagger}C_k^{(j)}\rho + \rho C_k^{(j)\dagger}C_k^{(j)}\right)\end{aligned} \tag{3}$$

for $j = A,B$ and $k = 1,2$. The Lindblad operators $C_1^{(j)} = \sqrt{\Gamma_e}|g_j\rangle\langle e_j|$ and $C_2^{(j)} = \sqrt{\Gamma_r}|g_j\rangle\langle r_j|$ have been introduced to describe decay processes of the jth atom via spontaneous emission. For our two-atom system, Eq. (3) becomes a set of dynamic equations for 9×9 density matrix elements $\rho_{mn,pq}$, with m and n denoting states of atom A and p and q denoting states of atom B.

In the following, we consider only a specific case where the pumping and coupling fields are modulated into two Gaussian pulses separated by a time delay τ so that we have the time-dependent Rabi frequencies

$$\begin{aligned}\Omega_p(t) &= \Omega_{p0}e^{-(t-t_{\text{end}}/2-\tau/2)^2/T_p^2}, \\ \Omega_c(t) &= \Omega_{c0}e^{-(t-t_{\text{end}}/2+\tau/2)^2/T_c^2},\end{aligned} \tag{4}$$

with t_{end} being the end time of both pulses, $T_{p,c}$ being the half widths, and $\Omega_{p0,c0}$ being the peak Rabi frequencies. We stress that the two light pulses will be applied in the counterintuitive order ($\tau > 0$), with their overlap satisfying the adiabatic criteria $\sqrt{\Omega_{p0}^2 + \Omega_{c0}^2} \gtrsim 10/\tau$ and $\tau \approx T_p + T_c$. Such criteria are attained as in Ref. [1] for independent atoms by considering that $\mathcal{V}_{ee}$, $\mathcal{V}_{rr}$, and $\mathcal{D}_{er}$ (comparable to or smaller than Ω_{p0} and Ω_{c0}) do not change the energy splitting of the relevant dressed states too much.

It is well known that single-atom Hamiltonians $\mathcal{H}_{A,B}$ have eigenstates $|D_{A,B}\rangle = [\cos\theta|g_{A,B}\rangle - \sin\theta|r_{A,B}\rangle]$, with $\tan\theta = \Omega_p/\Omega_c$ corresponding to zero eigenvalues $\lambda_{A,B} = 0$ on two-photon resonance ($\Delta = 0$). Such eigenstates naturally exclude the intermediate states $|e_{A,B}\rangle$ as required to answer for the perfect destructive interference between pathways $|g_{A,B}\rangle \leftrightarrow |e_{A,B}\rangle$ and $|e_{A,B}\rangle \leftrightarrow |r_{A,B}\rangle$. Single-photon detunings ($\Delta_p = -\Delta_c$) are irrelevant to $|D_{A,B}\rangle$, although they play an important role in attaining other eigenstates with nonvanishing eigenvalues. Consequently, the Hamiltonian in Eq. (1) has a (separable) product eigenstate of zero eigenvalue with $\Delta = 0$,

$$\begin{aligned}|D_0(t)\rangle = &[\cos\theta(t)|g_A\rangle - \sin\theta(t)|r_A\rangle] \\ &\otimes [\cos\theta(t)|g_B\rangle - \sin\theta(t)|r_B\rangle],\end{aligned} \tag{5}$$

in the absence of interatomic interactions ($\mathcal{V}_{ee} = \mathcal{V}_{rr} = \mathcal{D}_{er} = 0$). Then it is viable to transfer, via an adiabatic passage, the atomic population from the double ground state $|gg\rangle$ to the double Rydberg state $|rr\rangle$ without populating the single Rydberg state $|e\rangle$ of either atom. In the general case of $\Delta \neq 0$ and $\mathcal{V}_{ee},\mathcal{V}_{rr},\mathcal{D}_{er} \neq 0$, however, such a simple separable-state dynamics does not exist, yielding a very intractable entangled-state dynamics even in the case of adiabatic evolution. Therefore we should consider the more general two-atom eigenstate

$$\begin{aligned}|\psi(t)\rangle = &c_{gg}(t)|gg\rangle + c_{ge}(t)|ge\rangle + c_{gr}(t)|gr\rangle \\ &+ c_{eg}(t)|eg\rangle + c_{ee}(t)|ee\rangle + c_{er}(t)|er\rangle \\ &+ c_{rg}(t)|rg\rangle + c_{re}(t)|re\rangle + c_{rr}(t)|rr\rangle,\end{aligned} \tag{6}$$

with $|c_{ij}(t)|^2 = \rho_{ii,jj}(t)(i,j = g,e,r)$. In the next section, we will implement numerical calculations to examine the controlled population transfer and entanglement generation by solving $\rho_{ii,jj}(t)$ from Eq. (3).

III. RESULTS AND DISCUSSION

In this section, we adopt practical parameters for cold ^{87}Rb atoms to implement the numerical calculations mentioned above by considering $|g\rangle = 5S_{1/2}$, $|e\rangle = 70S_{1/2}$, and $|r\rangle = 70P_{3/2}$, with $\Gamma_e/2\pi = 2.6$ kHz and $\Gamma_r/2\pi = 1.0$ kHz [35]. The interactions $\mathcal{V}_{ee}$, $\mathcal{V}_{rr}$, and $\mathcal{D}_{er}$ between two such atoms separated by a 3.37 μm distance are approximately $2\pi \times \{100,200,100\}$ MHz, with $C_6^{ee} = 2\pi \times 140$ GHz μm^6, $C_6^{rr} = 2\pi \times 290$ GHz μm^6, and $C_3^{er} = 2\pi \times 3.8$ GHz μm^3 [29,32]. As to the counterintuitive sequence of pumping and coupling pulses, we choose in what follows $\Omega_{p0}/2\pi = \Omega_{c0}/2\pi = 100$ MHz, $t_{\text{end}} = 8$ μs, $\tau = 1.0$ μs, and $T_p = T_c = 1.0$ μs as relevant parameters.

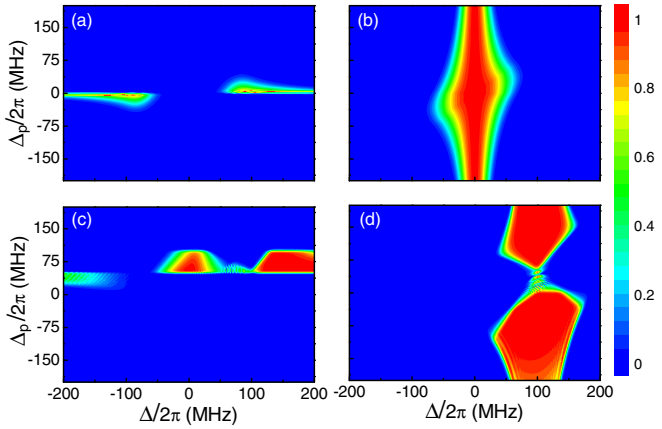

FIG. 2. (Color online) Double Rydberg excitations (a, c) $\rho_{ee,ee}$ and (b, d) $\rho_{rr,rr}$ as functions of single-photon detuning Δ_p and two-photon detuning Δ at time $t = 8\ \mu$s with relevant parameters given at the beginning of Sec. III. The two top (bottom) panels are attained in the absence (presence) of vdW and DDI interactions $\mathcal{V}_{ee}$, $\mathcal{V}_{rr}$, and $\mathcal{D}_{er}$.

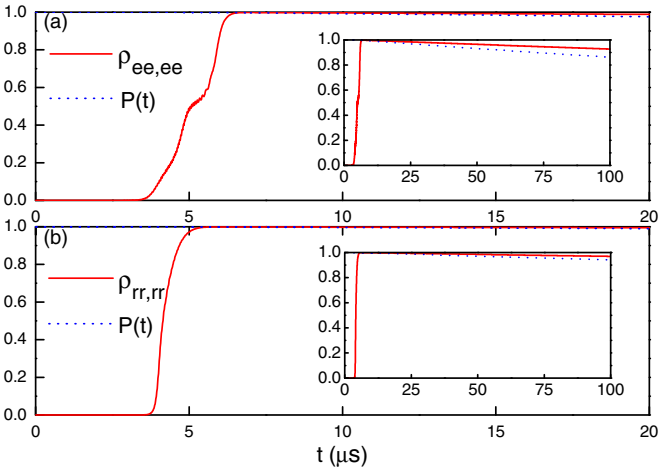

FIG. 3. (Color online) (a) Time evolution of the population in state $|ee\rangle$ and the purity $P(t) = \mathrm{Tr}[\rho^2(t)]$ in the antiblockade regime with $\Delta_p/2\pi = 58$ MHz and $\Delta/2\pi = 150$ MHz. (b) Time evolution of the population in state $|rr\rangle$ and the purity $P(t) = \mathrm{Tr}[\rho^2(t)]$ in the antiblockade regime with $\Delta_p/2\pi = -50$ MHz and $\Delta/2\pi = 100$ MHz.

A. Efficient population transfer

In Fig. 2 we plot double Rydberg populations $\rho_{ee,ee}$ and $\rho_{rr,rr}$ at the end of a pulse sequence ($t = 8\ \mu$s) as functions of single-photon detuning Δ_p and two-photon detuning Δ. From Figs. 2(a) and 2(b), we can see an efficient population transfer from the ground state $|g\rangle$ to the Rydberg state $|e\rangle$ ($|r\rangle$) near the single-photon (two-photon) resonance via STIRAP in the absence of interactions $\mathcal{V}_{ee}$, $\mathcal{V}_{rr}$, and $\mathcal{D}_{er}$. Comparing Fig. 2(a) with Fig. 2(c), we find that the region corresponding to an efficient double Rydberg excitation with $\rho_{ee,ee} \approx 1$ moves upward as the interatomic interactions are included. The underlying physics is twofold: (i) the vdW interaction $\mathcal{V}_{ee}$ can generate a large shift of state $|ee\rangle$ and then result in a blockade effect suppressing $\rho_{ee,ee}$ at $\Delta_p = 0.0$; (ii) a suitable single-photon detuning can compensate this level shift and then result in an antiblockade effect enhancing $\rho_{ee,ee}$ at $\Delta_p = \mathcal{V}_{ee}/2$. Similarly, the region corresponding to an efficient double Rydberg excitation with $\rho_{rr,rr} \approx 1$ moves rightward with its center located at $\Delta = \mathcal{V}_{rr}/2$ when the interatomic interactions are included. This implies that the antiblockade effect enhancing $\rho_{rr,rr}$ appears when a suitable two-photon detuning compensates the level shift caused by $\mathcal{V}_{rr}$, as shown in Figs. 2(b) and 2(d). It is also clear that the antiblockade region in the presence of interatomic interactions is larger than that in the absence of interatomic interactions.

To see how the two-atom system evolves in the antiblockade region, we plot in Fig. 3 the double Rydberg excitation $\rho_{ee,ee}$ ($\rho_{rr,rr}$) and the purity $P(t) = \mathrm{Tr}[\rho^2(t)]$ as a function of time t. After a careful parameter optimization, we choose $\Delta_p/2\pi = 58$ MHz and $\Delta/2\pi = 150$ MHz in the antiblockade region of state $|ee\rangle$ in Fig. 3(a); $\Delta_p/2\pi = -50$ MHz and $\Delta/2\pi = 100$ MHz in the antiblockade region of state $|rr\rangle$ in Fig. 3(b). As we can see, $\rho_{ee,ee}$ and $\rho_{rr,rr}$ gradually increase from 0.0 to approach 1.0 as the pumping and coupling fields are applied in a counterintuitive sequence. At the end of this pulse sequence ($t = 8\ \mu$s), we find $\rho_{ee,ee} = 0.9974$ and $P = 0.9949$ in Fig. 3(a), while $\rho_{rr,rr} = 0.9986$ and $P = 0.9974$ in Fig. 3(b). Both double Rydberg states $|ee\rangle$ and $|rr\rangle$ seem very stable since both single Rydberg states $|e\rangle$ and $|r\rangle$ have rather long lifetimes (small decay rates). This is evident as $\rho_{ee,ee}$ and $\rho_{rr,rr}$ reduce slowly after $t = t_{\mathrm{end}}$ together with purity $P(t)$ (see the insets). Briefly, one can achieve efficient population transfer to either Rydberg state by controlling single-photon and two-photon detunings to counteract the blockade effect.

B. Reliable entanglement generation

In Fig. 4 we show it is possible to generate three maximal entangled states via STIRAP in the presence of interactions

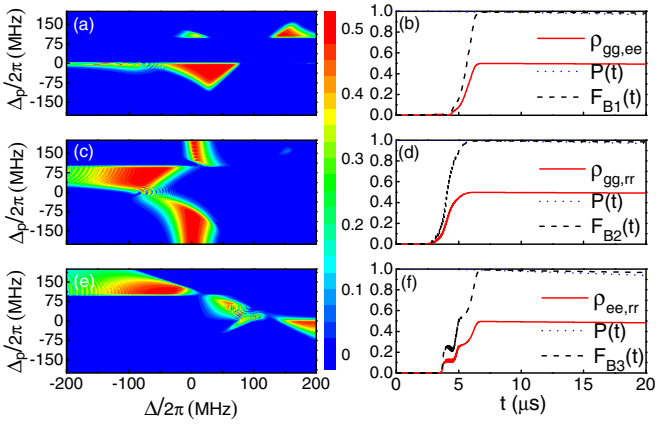

FIG. 4. (Color online) Populations (a) $\rho_{gg,ee}$, (c) $\rho_{gg,rr}$, and (e) $\rho_{ee,rr}$ as functions of single-photon detuning Δ_p and two-photon detuning Δ in the presence of interactions $\mathcal{V}_{ee}$, $\mathcal{V}_{rr}$, and $\mathcal{D}_{er}$ at time $t = 8\mu s$. Time evolution of populations (b) $\rho_{gg,ee}$ for $\Delta_p/2\pi = -20$ MHz and $\Delta/2\pi = 40$ MHz, (d) $\rho_{gg,rr}$ for $\Delta_p/2\pi = -120$ MHz and $\Delta/2\pi = 0.0$ MHz, and (f) $\rho_{ee,rr}$ for $\Delta_p/2\pi = 110$ MHz and $\Delta/2\pi = -42$ MHz together with the corresponding purities and fidelities.

$\mathcal{V}_{ee}$, $\mathcal{V}_{rr}$, and $\mathcal{D}_{er}$. In Fig. 4(a), $\rho_{gg,ee} = \rho_{ee,gg}$ are plotted as functions of single-photon detuning Δ_p and two-photon detuning Δ at the ending time ($t = 8$ μs). It is clear that we have $\rho_{gg,ee} = \rho_{ee,gg} \approx 0.5$ in a region near $\Delta_p/2\pi = -50$ MHz and $\Delta/2\pi = 0.0$ MHz, indicating $|c_{gg(gr,ee,er,rg,re,rr)}|^2 \approx 0.0$ and $|c_{ge(eg)}|^2 \approx 0.5$, so that state $|\psi\rangle$ in Eq. (6) reduces to either $|B_1\rangle = 1/\sqrt{2}(|ge\rangle + |eg\rangle)$ or $|D_1\rangle = 1/\sqrt{2}(|ge\rangle - |eg\rangle)$ in a good approximation. A further calculation of the fidelity $F_\psi(t) = \langle\psi|\rho(t)|\psi\rangle$ verifies that the two-atom system evolves, in fact, to $|B_1\rangle$ rather than $|D_1\rangle$ because we have $F_{B1}(t) \to 1.0$ and $F_{D1}(t) \to 0.0$. To better understand why only even-parity state $|B_1\rangle$ is attained, we should consider that both $|ge\rangle$ and $|eg\rangle$ originate from $|gg\rangle$ with either atom A or atom B excited to $|e\rangle$ from $|g\rangle$ and thus have an identical $\pi/2$ phase shift relative to $|gg\rangle$ after absorbing a single photon. In Fig. 4(b), population $\rho_{gg,ee}$, purity $P(t) = \mathrm{Tr}[\rho^2(t)]$, and fidelity $F_{B1}(t) = \langle B_1|\rho(t)|B_1\rangle$ are plotted as a function of time t with $\Delta_p/2\pi = -20$ MHz and $\Delta/2\pi = 40$ MHz. We find $\rho_{gg,ee} = 0.4992$, $P = 0.9973$, and $F_{B1} = 0.9982$ at $t = 8.0$ μs, and they decay very slowly after this ending time of both pumping and coupling pulses. In Figs. 4(c) and 4(e) we show plots of $\rho_{gg,rr}$ and $\rho_{ee,rr}$ similar to that in Fig. 4(a). We find in Fig. 4(c) $\rho_{gg,rr} \approx 0.5$ in a region near $\Delta/2\pi = 0.0$ MHz and $\Delta_p/2\pi < -100$ MHz or $\Delta_p/2\pi > 100$ MHz, which indicates an entangled state $|B_2\rangle = 1/\sqrt{2}(|gr\rangle + |rg\rangle$. We find in Fig. 4(e) $\rho_{ee,rr} \approx 0.5$ in a region near $\Delta/2\pi \approx -50$ MHz and $\Delta_p/2\pi \approx 100$ MHz, which indicates an entangled state $|B_3\rangle = 1/\sqrt{2}(|er\rangle + |re\rangle$. The dynamic generation and evolution of $|B_2\rangle$ and $|B_3\rangle$ are shown in Fig. 4(d), with $\Delta_p/2\pi = -120$ MHz and $\Delta/2\pi = 0.0$ MHz, and in Fig. 4(f), with $\Delta_p/2\pi = 110$ MHz and $\Delta/2\pi = -42$ MHz, respectively. We find $\rho_{gg,rr} = 0.4989$, $P = 0.9987$, and $F_{B2} = 0.9979$ for state $|B_2\rangle$, while $\rho_{ee,rr} = 0.4976$, $P = 0.9962$, and $F_{B3} = 0.9951$ for state $|B_3\rangle$ at the ending time $t = 8$ μs. Note that $|B_3\rangle$ has never been achieved before using dipole blockade and is of particular interest because it allows us, e.g., to generate a deterministic entangled photon pair from the two Rydberg states.

States $|B_1\rangle$, $|B_2\rangle$, and $|B_3\rangle$ are the same kind of Bell state $1/\sqrt{2}(|01\rangle \pm |10\rangle)$, but it is also viable to generate another kind of Bell state $1/\sqrt{2}(|00\rangle \pm |11\rangle)$. In Fig. 5(a), we plot $\rho_{gg,gg}$ as functions of single-photon detuning Δ_p and two-photon detuning Δ in the presence of interactions $\mathcal{V}_{ee}$, $\mathcal{V}_{rr}$, and $\mathcal{D}_{er}$ at the ending time $t = 8\mu$s. Comparing Fig. 5(a) with Fig. 2(c), we find that $\rho_{gg,gg} \approx 0.5$ and $\rho_{ee,ee} \approx 0.5$ near the position of $\Delta_p/2\pi = 0.0$ MHz. This indicates that the two-atom system evolves to state $|D_4\rangle = 1/\sqrt{2}(|gg\rangle - |ee\rangle)$ as identified by also calculating the fidelity of $F_{D4}(t) \to 1.0$. Here odd-parity state $|D_4\rangle$ instead of even-parity state $|B_4\rangle$ is attained simply because the simultaneous excitations of atom A and atom B from $|g\rangle$ to $|e\rangle$ result in a π phase shift of $|ee\rangle$ relative to $|gg\rangle$ after absorbing two photons. With a careful parameter optimization, we plot populations $\rho_{gg,gg}$ and $\rho_{ee,ee}$, purity $P(t)$, and fidelity $F_{D4}(t)$ as a function of time t with $\Delta_p/2\pi = 50$ MHz and $\Delta/2\pi = -1$ MHz in Fig. 5(b). We find $\rho_{gg,gg} = 0.4994$, $\rho_{ee,ee} = 0.4979$, $P = 0.9966$, and $F_{D4} = 0.9968$ at the ending time $t = 8$ μs. It is worth noting that the four entangled states shown above have rather high purities and fidelities and are very stable against atomic spontaneous decay.

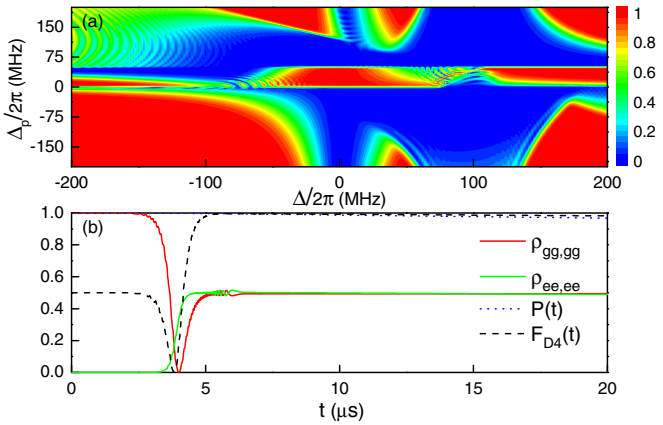

FIG. 5. (Color online) (a) Population $\rho_{gg,gg}$ as a function of single-photon detuning Δ_p and two-photon detuning Δ in the presence of interactions $\mathcal{V}_{ee}$, $\mathcal{V}_{rr}$, and $\mathcal{D}_{er}$ at time $t = 8\mu$s. (b) Time evolution of population $\rho_{gg,gg}$ for $\Delta_p/2\pi = 50$ MHz and $\Delta/2\pi = -1.0$ MHz together with the corresponding purity and fidelity.

Finally, we notice that mechanical forces among Rydberg atoms and the spread of atomic wave packets may cause increased decoherence in the excitation dynamics and essential particle losses out of the optical potentials [36,37]. This is relevant when the Rabi frequency of a pumping field is comparable to or several tens of the optical potential U_0 of a few recoil energies E_R (e.g., ~3.5 kHz for rubidium atoms) [36,37]. In our case, however, we have considered (i) the pumping and coupling fields are so strong that their Rabi frequencies greatly overwhelm the motional induced decoherence rates and (ii) the spread of atomic wave packets in much deeper potentials is so narrow that it is viable to neglect particle losses. So we expect that atomic motions just result in small uncertainties (e.g., ~0.5 MHz) in vdW and DDI potentials and will not evidently reduce the efficiency of population transfer and the fidelity of entanglement generation.

IV. CONCLUSIONS

In summary, we have studied the adiabatic passage for a pair of atoms driven into the three-level ladder configuration with two Rydberg states. We find that it is viable to achieve efficient atomic population transfer from the ground state to either Rydberg state or to implement stable maximal entangled states of high purities and fidelities by modulating single-photon and two-photon detunings in the presence of vdW and DDI potentials. An efficient atomic population transfer is attained when sufficiently large single-photon and two-photon detunings completely compensate the dipole-induced level shift of one Rydberg state. This is, in fact, the result of a perfect antiblockade effect, which allows a unit probability of Rydberg excitations of both atoms. A stable maximal entangled state is generated, however, when the moderately large single-photon and two-photon detunings partially compensate the dipole-induced level shift of one Rydberg state. This is, in fact, the result of an imperfect antiblockade effect, which allows a half probability of Rydberg excitations of both atoms. In particular,

we stress that state $|B_3\rangle$ involves two different Rydberg states and thus may be explored to attain deterministic entangled photon pairs. Finally, we expect that similar multipartite entanglements could be further attained if our scheme is extended to study three or more atoms, e.g., suitably arranged in optical lattices of dipole traps [38]. This is essential for the implementation of various protocols in quantum teleportation, cryptography, computation, etc.

ACKNOWLEDGMENTS

This work is supported by the National Natural Science Foundation (Grants No. 11174110 and No. 61378094) and the National Basic Research Program (Grant No. 2011CB921603) of China. The authors would like to thank the anonymous referee for valuable comments that have much improved the manuscript.

[1] K. Bergmann, H. Theuer, and B. W. Shore, Rev. Mod. Phys. **70**, 1003 (1998).
[2] D. Yan, C.-L. Cui, M. Zhang, and J.-H. Wu, Phys. Rev. A **84**, 043405 (2011).
[3] D. Petrosyan and K. Mølmer, Phys. Rev. A **87**, 033416 (2013).
[4] J. Qian, J.-J. Zhai, L. Zhang, and W.-P. Zhang, Phys. Rev. A **91**, 013411 (2015).
[5] D. Comparat and P. Pillet, J. Opt. Soc. Am. B **27**, A208 (2010).
[6] J. D. Pritchard, D. Maxwell, A. Gauguet, K. J. Weatherill, M. P. A. Jones, and C. S. Adams, Phys. Rev. Lett. **105**, 193603 (2010).
[7] M. Viteau, P. Huillery, M. G. Bason, N. Malossi, D. Ciampini, O. Morsch, E. Arimondo, D. Comparat, and P. Pillet, Phys. Rev. Lett. **109**, 053002 (2012).
[8] M. D. Lukin, M. Fleischhauer, R. Côté, L.-M. Duan, D. Jaksch, J. I. Cirac, and P. Zoller, Phys. Rev. Lett. **87**, 037901 (2001).
[9] D. Tong, S. M. Farooqi, J. Stanojevic, S. Krishnan, Y.-P. Zhang, R. Côté, E. E. Eyler, and P. L. Gould, Phys. Rev. Lett. **93**, 063001 (2004).
[10] K. Singer, M. Reetz-Lamour, T. Amthor, L. G. Marcassa, and M. Weidemüller, Phys. Rev. Lett. **93**, 163001 (2004).
[11] E. Urban, T. A. Johnson, T. Henage, L. Isenhower, D. D. Yavuz, T. G. Walker, and M. Saffman, Nat. Phys. **5**, 110 (2009).
[12] A. Gaëtan, Y. Miroshnychenko, T. Wilk, A. Chotia, M. Viteau, D. Comparat, P. Pillet, A. Browaeys, and P. Grangier, Nat. Phys. **5**, 115 (2009).
[13] L. Béguin, A. Vernier, R. Chicireanu, T. Lahaye, and A. Browaeys, Phys. Rev. Lett. **110**, 263201 (2013).
[14] C. Ates, T. Pohl, T. Pattard, and J. M. Rost, Phys. Rev. Lett. **98**, 023002 (2007).
[15] T. Amthor, C. Giese, C. S. Hofmann, and M. Weidemüller, Phys. Rev. Lett. **104**, 013001 (2010).
[16] J. Qian, X.-D. Zhao, L. Zhou, and W.-P. Zhang, Phys. Rev. A **88**, 033422 (2013).
[17] E. Brion, L. H. Pedersen, and K. Mølmer, J. Phys. B **40**, S159 (2007).
[18] M. Müller, I. Lesanovsky, H. Weimer, H. P. Büchler, and P. Zoller, Phys. Rev. Lett. **102**, 170502 (2009).
[19] L. Isenhower, E. Urban, X. L. Zhang, A. T. Gill, T. Henage, T. A. Johnson, T. G. Walker, and M. Saffman, Phys. Rev. Lett. **104**, 010503 (2010).
[20] X. L. Zhang, A. T. Gill, L. Isenhower, T. G. Walker, and M. Saffman, Phys. Rev. A **85**, 042310 (2012).
[21] I. I. Beterov, M. Saffman, E. A. Yakshina, V. P. Zhukov, D. B. Tretyakov, V. M. Entin, I. I. Ryabtsev, C. W. Mansell, C. MacCormick, S. Bergamini, and M. P. Fedoruk, Phys. Rev. A **88**, 010303(R) (2013).
[22] M. M. Müller, M. Murphy, S. Montangero, T. Calarco, P. Grangier, and A. Browaeys, Phys. Rev. A **89**, 032334 (2014).
[23] D. D. Bhaktavatsala Rao and K. Mølmer, Phys. Rev. A **89**, 030301(R) (2014).
[24] M. H. Goerz, E. J. Halperin, J. M. Aytac, C. P. Koch, and K. B. Whaley, Phys. Rev. A **90**, 032329 (2014).
[25] T. Keating, R. L. Cook, A. M. Hankin, Y.-Y. Jau, G. W. Biedermann, and I. H. Deutsch, Phys. Rev. A **91**, 012337 (2015).
[26] D. Møller, L. B. Madsen, and K. Mølmer, Phys. Rev. Lett. **100**, 170504 (2008).
[27] D. D. Bhaktavatsala Rao and K. Mølmer, Phys. Rev. Lett. **111**, 033606 (2013).
[28] S. Wüster, S. Möbius, M. Genkin, A. Eisfeld, and J. M. Rost, Phys. Rev. A **88**, 063644 (2013).
[29] D. D. Bhaktavatsala Rao and K. Mølmer, Phys. Rev. A **90**, 062319 (2014).
[30] M. Saffman and K. Mølmer, Phys. Rev. Lett. **102**, 240502 (2009).
[31] W.-B. Li, D. Viscor, S. Hofferberth, and I. Lesanovsky, Phys. Rev. Lett. **112**, 243601 (2014).
[32] D. Petrosyan and K. Mølmer, Phys. Rev. Lett. **113**, 123003 (2014).
[33] A. M. Hankin, Y.-Y. Jau, L. P. Parazzoli, C. W. Chou, D. J. Armstrong, A. J. Landahl, and G. W. Biedermann, Phys. Rev. A **89**, 033416 (2014).
[34] R. Löw, H. Weimer, J. Nipper, J. B. Balewski, B. Bütscher, H. P. Buchler, and T. Pfau, J. Phys. B **45**, 113001 (2012).
[35] See T. F. Gallagher, *Rydberg Atoms* (Cambridge University Press, Cambridge, 1994), p. 49, where an empirical formula $\tau = \tau_0 * n^\alpha$ has been used to calculate the decay rates $\Gamma_{e,r} = 2\pi/\tau_{e,r}$ with pertinent values of τ_0 and α.
[36] C. Ates, B. Olmos, W.-B. Li, and I. Lesanovsky, Phys. Rev. Lett. **109**, 233003 (2012).
[37] W.-B. Li, C. Ates, and I. Lesanovsky, Phys. Rev. Lett. **110**, 213005 (2013).
[38] D. Barredo, H. Labuhn, S. Ravets, T. Lahaye, A. Browaeys, and C. S. Adams, Phys. Rev. Lett. **114**, 113002 (2015).